Influence of microscopic composition on the strength of rock-like materials under various loading rates

Meng-Chia Weng
National Yang Ming Chiao Tung University, Hsinchu, Taiwan

Hoang-Khanh Le
National Yang Ming Chiao Tung University, Hsinchu, Taiwan

Hung-Hui Li
National Defense University, Hsinchu, Taiwan

Chih-Shan Lee
National Yang Ming Chiao Tung University, Hsinchu, Taiwan

Chia-Chi Chiu
National Taipei University of Technology, Taipei, Taiwan

ABSTRACT: This study investigated the dynamic strength and failure mode of rock-like materials considering the effect of microscopic composition and loading rate. A series of uniaxial compressive tests and SHPB tests were conducted on specimens, which contained 40% and 60% grain contents by volume and two types of cementation material (gypsum and weak gypsum). The results indicate a lower grain content and, correspondingly, a higher matrix volume, yields a higher quasi-static strength. The dynamic strength is related to not only the grain content but also the degree of grain breakage. Moreover, inter-granular fractures mainly occur under quasi-static compressive conditions, and the failure mode becomes trans-granular when the strain rate is high. Specimens with lower grain content exhibited fewer fractures and larger fragments than those with higher grain content. Considering the influence of matrix property, the weak-gypsum-cemented specimens exhibited higher dynamic increase factor and lower strength than the gypsum-cemented specimens.

Keywords: Rock-like material, spilt-Hopkinson pressure bar (SHPB) test, dynamic strength, strain rate.

1 INTRODUCTION

When rock-like materials are subjected to different types of external loadings, such as blasting, impact, earthquakes, and landslides, their strength and failure patterns are strongly influenced by loading rates (Zhao et al., 2014; Wisetsaen et al., 2015). Split Hopkinson Pressure Bar (SHPB) tests were commonly conducted to obtain the strain and stress of rock-like materials at high loading rates (Li and Shi, 2016; Yin et al., 2016). Many studies demonstrated that the rock strength increases with the strain rate, especially above 10^1 s^{-1} (Yao et al., 2017). Jeng et al. (2004) and Weng & Li (2012) investigate the influence of microscopic parameters on the mechanical properties of 13 types of sandstone in Taiwan. The results reveal that a lower porosity n and a lower grain area ratio GAR result in greater strength. GAR also affects fracture patterns. When GAR is low and the matrix is softer than the grains, inter-granular fractures are observed. Zhang & Zhao (2013) pointed out that inter-granular fracture is the main failure mode of marble under quasi-static compressive conditions. As the strain rate increases, the failure mode becomes trans-granular or intra-granular failure.

According to the aforementioned studies, rock strength and failure mode are influenced by both the grain content and loading rate, but the interaction between these two factors remains unclear. To clarify these influencing factors, a series of compressive tests and SHPB tests under various strain rates were performed herein. To control the microscopic composition and to reduce material uncertainties, artificial rock specimens, rather than real rock specimens, were used. The porosity of the adopted rock-like specimen is 14.8%, and the grain contents are 40% and 60%. Finally, the discrete element method (DEM) simulation was performed to evaluate the effects of grain content and loading rate on the dynamic response of the rock.

2 EXPERIMENT SETUP

2.1 Specimen preparation

To investigate systematically the influence of microscopic composition on the mechanical properties of sandstone, a series of rock-like specimens with grain contents, 40% and 60% by volume, were prepared. Artificial grains with a mean diameter of 5 mm were used as grains in rock. Each artificial grain was cast from Alumina, whose primary (approximately 99.6%) chemical constituent was Al_2O_3, which has a density γ of 2530 kg/m^3. The grain exhibited a high hardness (Mohs hardness = 7), high compressive strength (>100 MPa). Gypsum was chosen as the cementation material, and its uniaxial compressive strength and elastic modulus were 30.1 MPa and 6.0 GPa, respectively, and the strength and elastic modulus of the weak gypsum specimen were 15.2 MPa and 4.25 GPa, respectively. The strength and elastic modulus of the cementation material were much lower than those of the grains. For the tests at the low to medium strain rates (10^{-4} to 1 sec^{-1}), the cylinder specimens had a diameter of 50 mm and a height of 125 mm. The ratio of height to diameter was 2.5, consistent with the requirement of ISRM (1981). For the SHPB tests at a high strain rate (10^1 to 5.98×10^2 sec^{-1}), the specimens had a diameter of 40 mm and a height of 40 mm, resulting in a height-to-diameter ratio of unity (Figure 1a and 1b). The volume of cast mold for specimens of quasi-static and SHPB tests are 245,430, and 50,265 mm^3, respectively.

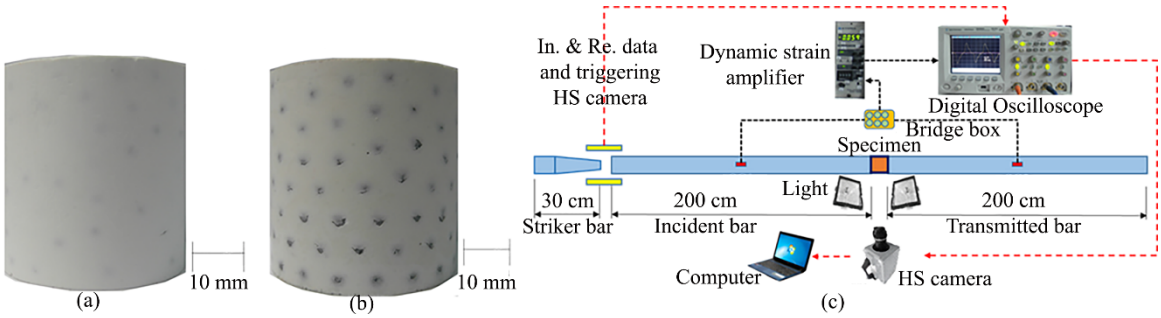

Figure 1. (a) Specimen with 40% grain content; (b) Specimen with 60% grain content; (c) Experimental setup of SHPB test and measurement system.

2.2 Apparatus and testing procedure

Two kinds of instrument were used to investigate the mechanical properties of the artificial rock specimens at various strain rates. In the tests at low to medium strain rates (10^{-4} to 1 sec^{-1}), a servo-controlled MTS 810 loading machine was used; in the tests at high strain rates (10^1 to 6.5×10^2 sec^{-1}), the SHPB apparatus was used. In the tests with the low to medium strain rates, the maximum capacity of the loading frame was 100 kN. The loading rates were set to 0.02, 0.2, 1.3, 13, and 100 mm/sec, corresponding to strain rates of 1×10^{-4}, 1×10^{-3}, 1×10^{-2}, 1×10^{-1}, and 1 sec^{-1}. The SHPB apparatus consisted of a compressed gas launcher, two long elastic bars, bearing and alignment fixtures, strain gages that were mounted on both bars, a data acquisition system, and control unit (Figure 1c). The elastic bar, which was composed of bearing steel, had a diameter of 40 mm and a length of 2000 mm. The Young's modulus of bearing steel is 208 GPa; its density is 7.85 g/cm^3, and

the theoretical wave velocity therein is 5131 m/s. In the tests at high strain rates, the gas pressure was set to 0.06, 0.1, 0.2, 0.3 and 0.4 MPa, and the corresponding strain rates range was 1×10^{2} to 5.98×10^{2} sec^{-1}. During the test, stress wave data were recorded, and a high-speed camera was utilized to capture images of the deformation and propagation of fracture of the specimen.

3 MECHANICAL BEHAVIOR OF ROCK AT VARIOUS STRAIN RATES

3.1 Strength and deformation modulus

Figure 2a plots the stress-strain curves of the gypsum-cemented specimen with 60% grain content at various strain rates (1×10^{-4} to 5.98×10^{2} sec^{-1}). The axial strain curves are generally linear in the pre-peak stage, and the initial modulus and strength increase with the strain rate. The peak strength ranges from 8.7 to 60.6 MPa and the peak strains are 0.3-1.4 %. At a low strain rate (10^{-2} sec^{-1}), the compressive strength was 11.1 MPa and the elastic modulus was 2.07 GPa, so the adopted artificial rock could be classified as low-strength rock, similar with those of Jeng et al. (2004). Similarly, the test result for specimens with 40% grain content is shown in Figure 2b. The peak strength ranges from 18.3 to 90.9 MPa, which is larger than that of specimens with 60% grain content, especially under high strain rates. The influence of the grain content and strain rate on the strength and failure mechanism of rock-like specimens is further investigated in the next section.

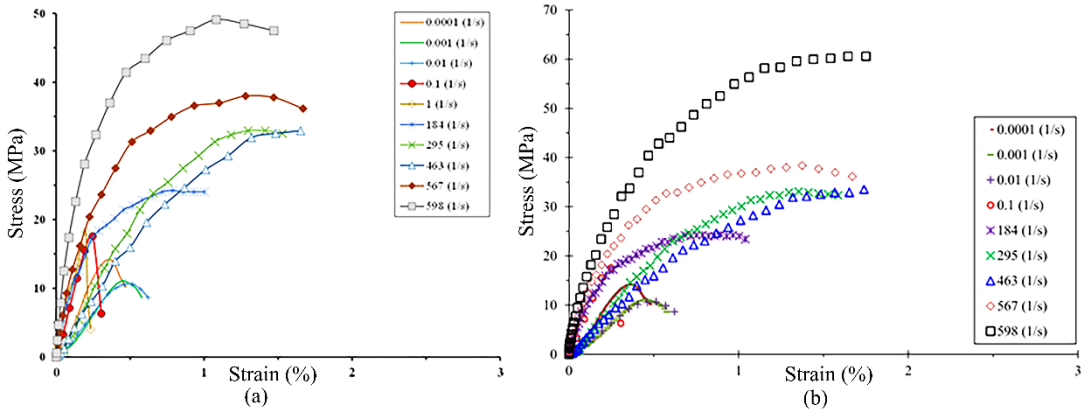

Figure 2. Test result of gypsum-cemented specimen under different microscopic compositions: (a) 60% grain content; (b) 40% grain content.

3.2 Failure pattern

Figure 3a presents the failure patterns of the gypsum-cemented specimen with 60% grain content at different strain rates (1×10^{-3} to 5.98×10^{2} sec^{-1}). Under strain rates 1×10^{-3} to 1 sec^{-1}, the specimens exhibited a main inclined shear fracture and several minor vertical fractures. The grains remained intact, and fractures were initiated from the interface of grain and gypsum. The angle of inclination between the main fracture and the loading direction decreases as the strain rate increases, so the developed main fracture is closer to vertical under a higher strain rate. This finding is consistent with results for real sandstone (Zhang & Zhao, 2014). In SHPB tests under strain rates of 2.95×10^{2} to 5.98×10^{2} sec^{-1}, the specimens exhibited quite different failure patterns. Rather than a main inclined fracture, numerous tiny linear or cruciform fractures initiated at the grain surface, and these fractures propagated until they coalesced. Ultimately, the specimen became heavily fragmented as a result of the coalesced fractures. Figure 3b shows the failure patterns of specimens with 40% grain content under different strain rates (1×10^{-4} sec^{-1} to 5.24×10^{2} sec^{-1}). Under strain rates of 1×10^{-4} sec^{-1} to 1 sec^{-1}, the specimens did not exhibit a main inclined fracture, as in Figure 3a, but exhibited numerous parallel splitting fractures, which developed in the matrix between grains. As strain rates increased above 2.56×10^{2} sec^{-1}, several parallel fractures initially developed and then propagated until they coalesced. Finally, each specimen was severely fragmented owing to the coalescence of

fractures. Most of the fractures in specimens with a 40% grain content initiated from the two ends of the specimen, instead of the grain boundaries as in specimens with a 60% grain content.

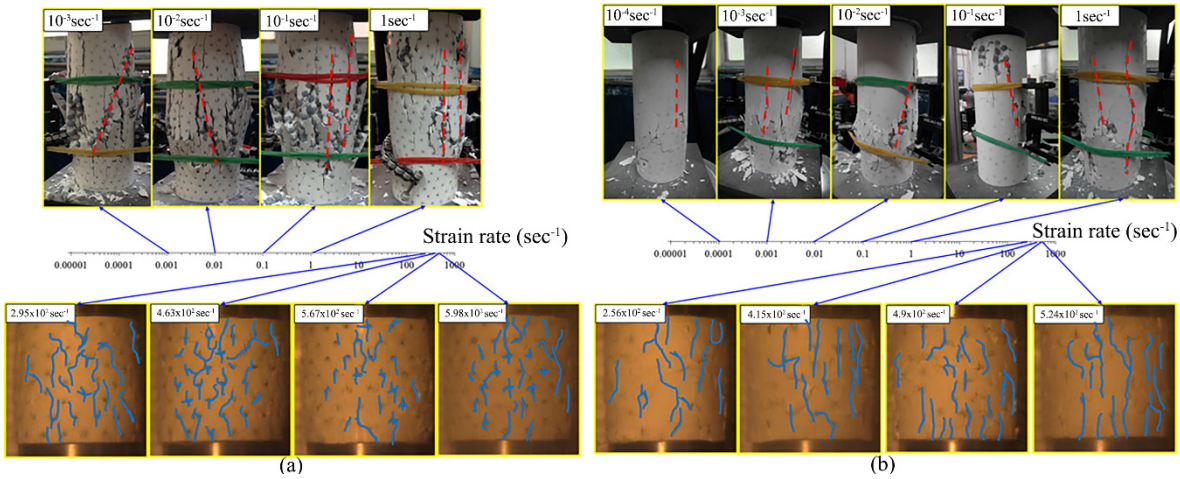

Figure 3. (a) Failure patterns of gypsum-cemented specimen under different microscopic compositions: (a) 60% grain content; (b) 40% grain content.

4 EFFECT OF MICROSCOPIC FACTORS ON STRENGTH

4.1 Effect of grain content

To evaluate further the degree of grain breakage of the failed specimen, sieve analysis was carried out: the broken grains were sieved out, and their weight percentage was measured. A series of sieves, #4-#20 (4.76 mm-0.841 mm), were used to separate the intact grain, grain fragments, and gypsum. The colors of grain and gypsum were quite different, so the grain fragment could be easily taken out. To quantify the grain fragments, the percentage of trans-granular failure (TG) is defined as

$$TG = \frac{W_F}{W_T} \times 100\% \quad (1)$$

where W_T and W_F are the weights of all grains and of the grain fragments, respectively.

Figure 4 compares the strengths of specimens with 60% and 40% grain contents at various strain rates. The strengths of specimens with 40% grain contents, ranging from 18.3 to 90.9 MPa, are obviously higher than those of the specimens with 60% grain content (Figure 4a). These results seem to demonstrate that higher grain content yields lower strength. However, the pure gypsum specimen, which contains no grains, exhibits the highest strength at a low strain rate, whereas the specimens with a 40% grain content exhibited the highest strength at a high strain rate. The grain content is not the only influencing factor on strength under various strain rate. To identify possible causes of the increase in strength at a high strain rate, Figure 4 also plots the variation of TG percentage. As for specimens with a 60% grain content, the TG percentage of those with 40% grain content remained zero at low strain rate, increasing to 5.42 % as the strain rate increased to 5.24×10^{2} sec^{-1}. These results reveal that a lower grain content and, correspondingly, larger matrix volume, provides higher quasi-static strength, but the dynamic strength is affected by not only the grain content but also the degree of grain breakage (TG percentage). A higher TG percentage induces a higher dynamic strength.

Figure 4b further shows the variation of the dynamic increase factor (DIF) with strain rate. The dynamic increase factor (DIF) is defined as the ratio of the dynamic strength to the quasi-static strength (strain rate of 1×10^{-4} sec^{-1}). In the strain rate range of 1×10^{-4} sec^{-1} to 1 sec^{-1}, the DIF of specimens with the 60% grain content ranged from 1 to 1.74, and that of specimens with the 40% exhibited similar values. The DIFs of specimens with both 60% and 40% grain contents increased

steeply with the strain rate above 1.84×10^2 sec^{-1}. As the strain rate increased to 5.3×10^2 sec^{-1}, the DIFs of specimens with 60% and 40% grain contents reached their highest values, which were 4.1 and 5.2, respectively, and the TG percentages reached their highest values, which were 8.88 % and 5.42 %, respectively. The DIF variation of the pure gypsum specimen with strain rate was insignificant, ranging from 1 to 1.52.

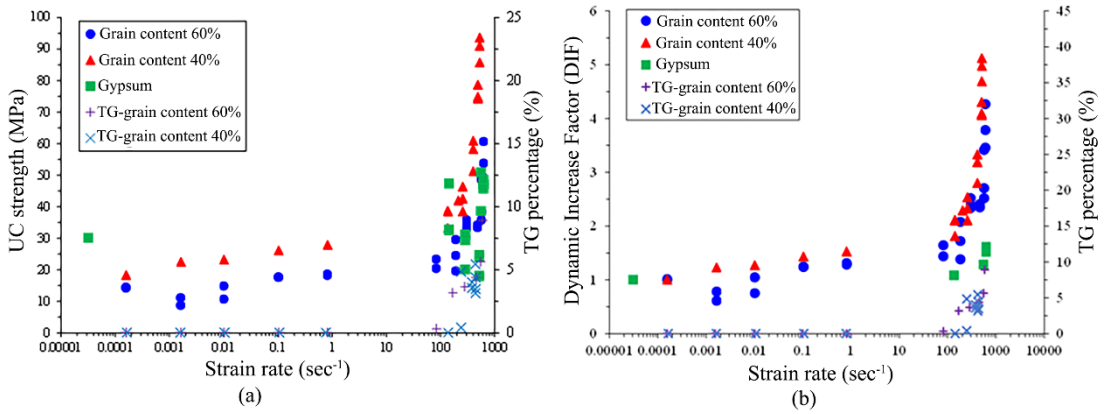

Figure 4. Comparison of strengths, TG percentages and DIFs of specimens with 60% and 40%: (a) Uniaxial compressive strength; (b) Dynamic increase factor (DIF).

4.2 Effect of matrix properties

Two types of cement, gypsum and weak gypsum, were used to investigate the effect of matrix bonding strength on rock strength. Figure 5 shows the strength variations of specimens with a 60% grain content and two cementing materials under various strain rates. Figure 5 also compares the strengths of pure gypsum and weak gypsum without any grains. The strengths of the weak-gypsum-cemented specimen, ranging from 6.7 to 41.0 MPa, were lower than those of the gypsum-cemented specimen, ranging from 8.7 to 60.6 MPa (Figure 5a). Figure 5b plots the variations of the DIFs of two matrices. In the strain rate range of 1×10^{-4} sec^{-1} to 1 sec^{-1}, the DIF of the gypsum-cemented specimen increased from 1 to 1.28 and that of the weak-gypsum-cemented specimen was higher, increasing from 1 to 1.74. The DIFs of both cemented specimens increased steeply with the strain rate above 8.2×10^2 sec^{-1}. When the strain rate increased to 5.9×10^2 sec^{-1}, the DIFs of the two cemented specimens were highest, at 4.1 and 7.9, respectively. Due to the low bonding strength of weak gypsum, the weak-gypsum-cemented specimen had a higher DIF than the gypsum-cemented specimen.

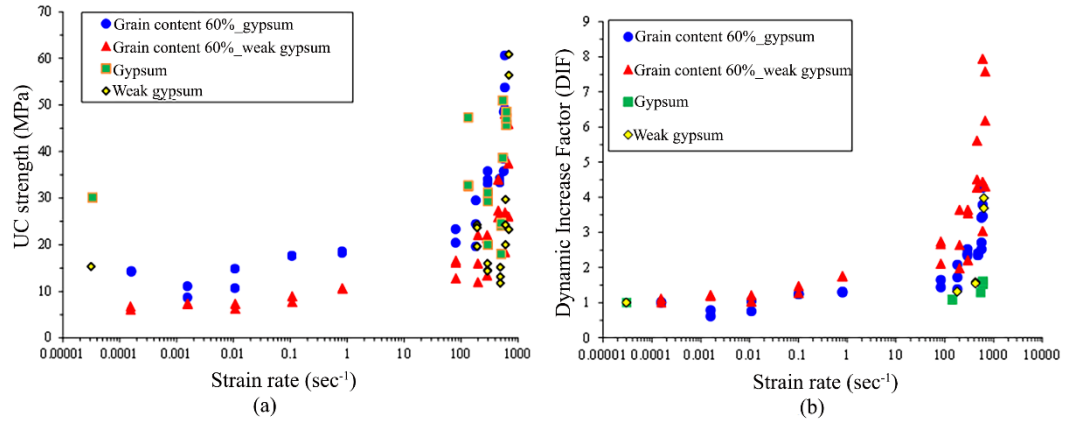

Figure 5. Variations of strength, DIF, and TG percentage of specimens with different cementing materials (60% grain content): (a) Uniaxial compressive strength; (b) Dynamic increase factor (DIF).

5 CONCLUSION

To investigate the of microscopic factors and loading rate on the strength and failure mode of rock, a series of uniaxial compressive tests and SHPB tests were performed. To control the microscopic composition and reduce the material uncertainties, artificial rock specimens were used. Two grain packing arrangements with 40% and 60% grain contents by volume, and two types of cement, gypsum and weak gypsum, were used to reflect the compositions of real rock. The results of the test were analyzed to elucidate the effects of grain content, matrix properties, and loading rate on the dynamic response of rock, including strength and failure patterns.

The test results show that a lower grain content, which corresponds to a larger matrix volume, yields a higher quasi-static strength (at strain rates from 10^{-5} to 10^{-1} sec^{-1}), whereas the dynamic strength (strain rates from 1×10^{2} sec^{-1} to 5.98×10^{2} sec^{-1}) are affected by not only the grain content but also the degree of grain breakage, which is denoted as TG percentage. Increasing the strain rate increased the TG percentage, which caused the greater strength.

Considering the influence of matrix property, the strengths of weak-gypsum-cemented specimens are lower than those of gypsum-cemented specimens. However, weak-gypsum-cemented specimens exhibited higher DIFs than the gypsum-cemented specimens. For the failure patterns, the inter-granular fractures occurred mostly under quasi-static compressive conditions, and the failure mode became trans-granular when the strain rate became high. In tests at high strain rates, specimens with 40% grain content exhibited fewer fractures and larger fragments than those with 60% grain content.

ACKNOWLEDGEMENTS

This research was financially supported by the Ministry of Science and Technology, Taiwan under Contract MOST 106-2625-M-390-001, MOST 107-2625-M-009-010, and MOST 108-2628-E-009 -004 -MY3.

REFERENCES

ISRM 1981. *Rock Characterization, Testing and Monitoring, ISRM suggested methods*. ed. E.T. Brown. publ. Pergamon Press, Oxford. 211

Jeng, F.S., Weng, M.C., Lin, M.L., & Huang, T.H. 2004. Influence of petrographic parameters on geotechnical properties of Tertiary sandstones from Taiwan. *Eng Geol* 73: 71-91.

Li, H.Y., & Shi, G.Y. 2016. A dynamic material model for rock materials under conditions of high confining pressures and high strain rates. *Int J Imp Eng* 89: 38-48.

Weng, M.C., & Li, H.H. 2012. Relationship between the deformation characteristics and microscopic properties of sandstone explored by the bonded-particle model. *Int J Rock Mech Min Sci* 56, 33-43.

Wisetsaen, S., Walsri, C., & Fuenkajorn, K. 2015. Effects of loading rate and temperature on tensile strength and deformation of rock salt. *Int J Rock Mech Min Sci* 73: 10-14.

Yao, W., Xu, Y., Yu, C.Y., & Xia, K.W. 2017. A dynamic punch-through shear method for determining dynamic Mode II fracture toughness of rocks. *Eng Frac Mech* 176: 161-177.

Yin, T.B., Shu, R.H., Li, X.B, Wang, P., & Dong, L.J. 2016. Combined effects of temperature and axial pressure on dynamic mechanical properties of granite. *Transactions of Nonferrous Metals Society of China* 26(8): 2209-2219.

Zhang, Q.B., & Zhao, J. 2013. Determination of mechanical properties and full-field strain measurements of rock material under dynamic loads. *Int J Rock Mech Min Sci* 60: 423-439.

Zhao, Y., Zhao, G.F., Jiang, Y., Elsworth, D., & Huang, Y. 2014. Effects of bedding on the dynamic indirect tensile strength of coal: laboratory experiments and numerical simulation. *International J Coal Geo* 132: 81-93.